Research Square

Preprints are preliminary reports that have not undergone peer review.
They should not be considered conclusive, used to inform clinical practice,
or referenced by the media as validated information.

Clinical and Functional Characterization of Three Homozygous NTRK1 Variants and A Brief Comparison of the Literature

Aydeniz Aydin Gumus

aydeniz.aydingumus@saglik.gov.tr

İstanbul Başakşehir Çam ve Sakura Şehir Hastanesi

Ekrem Akbulut

Malatya Turgut Özal Üniversitesi

Serdar BOZLAK

İstanbul Başakşehir Çam ve Sakura Şehir Hastanesi

Melih Civan

İstanbul Başakşehir Çam ve Sakura Şehir Hastanesi

Merve Cakmak

İstanbul Başakşehir Çam ve Sakura Şehir Hastanesi

Peren Perk

İstanbul Başakşehir Çam ve Sakura Şehir Hastanesi

Research Article

Keywords: pain, insensitivity, NTRK1, mutation, function

Posted Date: November 4th, 2026

DOI: https://doi.org/10.21203/rs.3.rs-11330579/v1

License: This work is licensed under a Creative Commons Attribution 4.0 International License.
Read Full License

Additional Declarations: No competing interests reported.

Abstract

Background

Loss-of-function variants in the NTRK1 gene, which encodes the NGF receptor TrkA, cause Hereditary Sensory and Autonomic Neuropathy IV (HSAN4/CIPA), a rare autosomal recessive disorder. Clinical heterogeneity among HSAN4/CIPA patients suggests that distinct variant types exert qualitatively different effects on TrkA structure and function. This study investigated the structural, functional, and clinical implications of three NTRK1 variants—p.His569Gln, p.Glu590Gln, and c.1177 + 2T > A—identified in five patients presenting with variable HSAN4/CIPA phenotypes.

Methods

Computational structural analyses, including rotamer scanning, DynaMUT2 stability predictions, and in silico splicing tools (MaxEntScan, SpliceAI), were employed to characterize each variant.

Results

The p.His569Gln, located within the kinase domain adjacent to the kinase insert domain (KID), increased TrkA stability ($\Delta\Delta G$ + 0.37 kcal·mol^{-1}), restricted conformational flexibility, and disrupted the αC-in arrangement and activation loop dynamics essential for NGF-induced signaling, consistent with a severe loss-of-function profile. p.Glu590Gln, situated at the ATP-binding hinge region, preserved backbone-mediated ATP contacts while subtly modulating local polarity and hydration through tolerable rotamer rearrangements, supporting a hypomorphic, partial loss-of-function effect concordant with a milder clinical presentation. The c.1177 + 2T > A splice donor variant disrupted the canonical GU dinucleotide at the + 2 position, predicted to near-completely abrogate normal splicing via exon skipping, cryptic donor activation, or intron retention, yielding a functionally null allele.

Conclusion

These findings indicate that the clinical severity of *NTRK1*-associated pain insensitivity disorder is associated with the location of the mutation, its molecular consequences, and functional outcomes; this provides a mechanistic framework for the correlations observed in *NTRK1*-associated pain insensitivity and contributes to the development of mutation-specific diagnostic and treatment strategies.

Introduction

Hereditary Sensory and Autonomic Neuropathy IV (HSAN4/CIPA) is a rare autosomal recessive disorder characterized by inability to perceive pain, anhidrosis, recurrent fevers, self-mutilating injuries, and variable cognitive impairment, caused by loss-of-function mutations in *NTRK1*, which encodes TrkA, the

high-affinity receptor tyrosine kinase for nerve growth factor (NGF)[1]. NTRK1 belongs to the tropomyosin receptor kinase (TRK) family, which governs the development and maintenance of nervous system function, and is a 25-kb, 17-exon gene located at 1q23.1[2]. NGF binding to TrkA triggers receptor autophosphorylation, supporting the survival, differentiation, and maintenance of nociceptive sensory and sympathetic cholinergic neurons[3]. *NTRK1* mutations typically disrupt the NGF-binding receptor structure, impairing this autophosphorylation and downstream signaling, which causes peripheral pain-sensing (C) fibers and sweat-gland-innervating sympathetic neurons to fail to develop or to degenerate—producing the hallmark pain insensitivity and anhidrosis of HSAN4/CIPA[4]. Clinically, this disorder is marked by profound pain insensitivity, often impaired temperature sensation, anhidrosis, heat intolerance, recurrent fractures, self-mutilation, joint destruction, chronic infections due to painlessness, and generalized sensory-sympathetic neuropathy on nerve studies/histology[5].

Material-Methods

This study included five patients and their asymptomatic family members, all born to consanguineous (first-cousin) parents: a 15-year-old male (P1) with recurrent ankle fractures; three brothers aged 7, 9, and 11 (P2–P4) with recurrent ankle fractures, reduced pain perception, and ankle deformities; and a 13-year-old female (P5) with recurrent osteomyelitis and scoliosis. DNA extracted prepheral blood samples were underwent whole-exome sequencing on the MGI T7 platform with the Twist WES kit with an average read depth of at least 130x. Variant data were evaluated by quality score; clinically significant, low-frequency variants from GnomAD were classified per ACMG guidelines[6]. The three homozygous *NTRK1* variants identified across the five patients were confirmed by Sanger sequencing, using primers designed from the patients' and family members' DNA.

The wild-type (wt-) and mutant (mt-) protein models for *NTRK1*(NM_002529.4) were created using Swiss-Model and AlphaFold3[7, 8]. Template-dependent modular domain modeling attempts utilized 4F0I, 2IFG, and 4PMP as templates[9–11]. Protein homology model quality assessments were performed using ProSA and Molprobity[12, 13] The changes in TrkA structure and stability caused by mutations were analyzed using DynaMUT2[14]. The deep convolutional neural network algorithm and MaxEntScan (Maximum Entropy Scan) were used to analyze the effects of the *NTRK1*(NM_002529.4):c.1177 + 2T > A mutation on the splice donor site in *NTRK1*[15, 16]. The rotamer-screened, geometry-based (heavy-atom) clash and H-link candidate analysis for the *NTRK1* mutations c.1707C > G:p.His569Gln and c.1768G > C:p.Glu590Gln was performed using Python (Biopython).

Results

P1, who had no laboratory abnormalities, was found by WES to be homozygous for NTRK1 (NM_002529.4):c.1707C > G p.(His569Gln), confirmed by Sanger sequencing (Fig. 1a); although he reportedly sweated heavily enough to require changing pajamas at night, he was unable to perceive heat or cold. Three brothers aged 7, 9, and 11 (P2–P4), followed by pediatric orthopedics for recurrent ankle fractures and foot deformities due to delayed healing, also reported thermal hypoesthesia, hypohidrosis,

episodic hyperthermia, and recurrent upper respiratory tract infections (averaging 20–25 episodes annually); WES showed them to be homozygous for *NTRK1* (NM_002529.4):c.1768G > C p.(Glu590Gln), with carrier status confirmed in both parents (Fig. 1b). P5, a 13-year-old female with unexplained neonatal fever, inability to sweat until age seven, two episodes of osteomyelitis, and scoliosis, was homozygous for *NTRK1* (NM_002529.4):c.1177 + 2T > A, with heterozygous carrier status confirmed in her parents and asymptomatic brother (Fig. 1c). Interpretations of the patients' variants are summarized in Table 1, and the associated clinical findings of HSAN4/CIPA are summarized in Table 2.

Table 1
NTRK1 variants found in patients

Patient	Variation	Zygosity	ACMG	GnomAD v4.1.1 Frequency
P1	*NTRK1*(NM_002529.4):c.1707C > G p.(His569Gln)	Homozygous	PM2, PP3	None *(Fraction of individuals with coverage over 30 in genome: 0.7)*
P2	*NTRK1*(NM_002529.4):c.1768G > C p.(Glu590Gln)	Homozygous	PM2,PM5,PP3	None *(Fraction of individuals with coverage over 30 in genome: 0.7)*
P3	*NTRK1*(NM_002529.4):c.1768G > C p.(Glu590Gln)	Homozygous	PM2,PM5,PP3	None *(Fraction of individuals with coverage over 30 in genome: 0.7)*
P4	*NTRK1*(NM_002529.4):c.1768G > C p.(Glu590Gln)	Homozygous	PM2,PM5,PP3	None *(Fraction of individuals with coverage over 30 in genome: 0.7)*
P5	*NTRK1* NM_002529.4 c.1177 + 2T > A	Homozygous	PM2, PVS1	None *(Fraction of individuals with coverage over 30 in genome: 0.6)*
PM2: Classified as moderately pathogenic based on extremely low allele frequency in the gnomAD population database.				
PM5: Classified as moderately pathogenic based on an amino acid substitution at a residue previously reported to harbor a distinct pathogenic variant				
PP3: All computational prediction tools consistently indicate a deleterious effect of this missense/splicing region variant on gene function.				
PVS1: A loss-of-function variant identified in a gene for which haploinsufficiency or null alleles are an established disease mechanism				

Table 2
Examination of clinical findings in patients with CIPA/HSAN4

Clinical Findings	**P1**	**P2**	**P3**	**P4**	**P5**
Age	15	7	9	11	13
Gender	Boy	Boy	Boy	Boy	Girl
Eye Finding	N	N	N	N	N
Mouth Accidental injury and ulceration of the lips and tongue due to decreased sensation	N	+	+	+	-
Vascular - Postural hypotension with compensatory tachycardia	N	N	N	N	N
SKELETAL - Neuropathic arthropathy - Osteomyelitis	+	+	+	+	+
Anhidrosis	N	+	+	+	+
Thick, calloused skin	+	+	+	+	+
Dystrophic nails	N	N	N	N	N
Hypotrichosis of the scalp	N	N	N	N	N
Developmental delay	N	N	N	N	N
Pain insensitivity, diffuse (including to visceral pain)	+	+	+	+	N
Temperature insensitivity, diffuse	+	+	+	+	+
Hyperactivity	+	+	+	+	N
Emotional lability	+	+	+	+	+
Fever, episodic, severe	N	N	N	N	N
Delayed wound healing with normal immune system	+	+	+	+	+
Increased susceptibility to severe and frequent infections with Staphylococcus aureus	+	+	+	+	+

Two-point discrimination testing in the three siblings (P2–P4) showed thresholds exceeding age-expected values across all regions, most pronounced distally and in the lower extremities—a pattern consistent with distal-predominant, length-dependent sensory neuropathy. The concordance among siblings suggests a hereditary etiology, while higher thresholds in the oldest sibling suggest a progressive course; P1's refusal of two-point discrimination testing was a limitation of this study. P5 had

normal two-point discrimination thresholds and normal electromyography, performed to exclude deep sensory involvement (results in Table 3). Psychiatric evaluation identified an impulse control disorder in P1, for which he is currently receiving therapy.

Table 3
Patients' two-point discrimination test results

2-point discrimination test areas	P2	P3	P4	P5
Tip of the index finger	**11 mm**	**11 mm**	**13 mm**	**5 mm**
Tip of the thumb	11 mm	11 mm	12 mm	6 mm
Palm (thenar region)	17 mm	18 mm	18 mm	10 mm
The back of the hand	31 mm	33 mm	34 mm	25 mm
Tip of the Hallux	**23 mm**	**25 mm**	**25 mm**	**15 mm**
The sole of the foot	25 mm	27 mm	28 mm	20 mm
The top of the foot	38 mm	41 mm	42 mm	25 mm

The TrkA protein homology models generated for p.His569Gln and p.Glu590Gln met the quality limits for X-ray diffraction (Fig. 2). The Z-scores ranged from − 9.49 to -6.94. The MolProbity scores ranged from 1.15 to 1.22. The mutations caused changes in the structure and stability of the TrkA. The p.His569Gln mutation increased TrkA stability ($\Delta\Delta G^{stability}$ 0.37 kcal.mol^{-1}). The tertiary structure stability provided by seven hydrophobic, five aromatic, and three polar interactions in wt-TrkA (Fig. 3a) was enhanced to ten hydrophobic, a hydrogen, two van der Waals, and a polar interactions in mt-TrkA (Fig. 3b). The interaction network established in wt-TrkA at position 569 with Tyr640, His571, and Ile572 has been expanded in mt-TrkA with the addition of two new residues (Ala636 and Gly637).The p.Glu590Gln mutation reduced TrkA stability ($\Delta\Delta G^{stability}$ -0.47 kcal.mol^{-1}). Tertiary structure stability, provided by seven polar, seven hydrophobic interactions, a van der Waals bond, and a hydrogen bond in wt-TrkA (Fig. 3c), was reduced to four hydrophobic and one polar interaction in mt-TrkA (Fig. 3d). The interaction network established with Val573, Arg574, Phe576, Met592, and Lys665 at position 590 in wt-TrkA narrowed in mt-TrkA due to the disappearance of interaction with the Val573 and Lys665 residues.

The c.1177 + 2T > A variant is located in the canonical 5' splice donor region (+ 2 position) of *NTRK1*. The + 1 and + 2 positions in the splice donor region form the conserved GU sequence in the vast majority of introns and are critical for U1 snRNP binding. This T > A change can disrupt this conserved motif and lead to slicing errors. MaxEntScan 5’ splice site analysis showed that the c.1177 + 2T > A variant significantly attenuated the canonical donor signal (wt: 5.196, mt: −2.987, Δ = −8.183). The splice site analysis using a deep evolutionary neural network algorithm (Splice AI) revealed a strong donor loss pattern (Δ = 0.97). This strongly supports the possibility of aberrant splicing (cryptic donor use/exon skipping/intron retention) (Fig. 4).

We performed a rotamer-screened, geometry-based (heavy-atom) assessment for His569Gln and Glu590Gln. Only the side-chain rotamers of Gln were systematically sampled (χ1, χ2, χ3; 18 combinations), while the backbone was kept fixed. Two readouts were evaluated for each rotamer: (i) steric compatibility/clashes, defined using a van der Waals overlap criterion (contacts counted as clashes when the interatomic distance satisfied $d < r_{sum} - 0.4$ Å), and (ii) candidate hydrogen bonds, inferred from heavy-atom geometry (no explicit hydrogens) using the thresholds D–A ≤ 3.3 Å and an approximate angular requirement ≥ 120°. For each rotamer, neighboring atoms within a 6 Å shell around the Gln side-chain atoms (CB/CG/CD/OE1/NE2) were scanned, and rotamers were ranked by "fewest clashes → lowest maximum overlap → highest number of H-bond candidates. The two substitutions show distinct local structural tolerability. At position 569, His→Gln accommodates only a limited number of low-clash rotamers, requiring constrained side-chain orientations achieved primarily through repacking rather than compensatory hydrogen bonding—reflecting a tightly packed, conformationally sensitive environment. In contrast, Glu590Gln accommodates multiple low-clash rotamers with geometrically plausible hydrogen bonding between OE1/NE2 groups and neighboring O/N atoms. Collectively, these findings indicate greater local structural tolerability for Glu590Gln than for the more conformationally restrictive His569Gln substitution.

Discussion

TrkA, encoded by NTRK1, is a high-affinity receptor for nerve growth factor (NGF) critical for the development and survival of nociceptive sensory neurons and sympathetic ganglia; loss-of-function mutations in *NTRK1* cause pain insensitivity and anhidrosis[17]. This study analyzed the structural and functional effects of three NTRK1 mutations (p.His569Gln, p.Glu590Gln, and c.1177 + 2T > A), which affect different regions of the TrkA protein and lead to significant differences in clinical phenotype.

TrkA is a type I tyrosine kinase receptor with distinct structural domains from N- to C-terminus (Fig. 2a). Its extracellular portion contains five domains: a central leucine-rich domain (domain 2) flanked by two cysteine-rich domains (domains 1 and 3), followed by two immunoglobulin-like domains (domains 4 and 5) responsible for neurotrophin binding, with domain 5 particularly critical for ligand binding and specificity. A single transmembrane helix connects this extracellular portion to the cytosolic side, where the intracellular tyrosine kinase domain comprises an N-lobe (mostly β-structured), a C-lobe (α-helical), and a connecting hinge region (Fig. 2b,c).

Within the kinase domain, the activation loop (DFG motif and activation segment), αC-helix, and intervening KID (kinase insert domain) are critical regulators of structure and function[9]. The p.His569Gln variant in the TrkA kinase N-lobe lies near the critical αC-helix/Lys axis, a region highly sensitive to local packing and conformational stability. Even low-clash rotamer conformations typically yield only adequate geometries, insufficient to maintain a robust hydrogen bond network. This disruption compromises the finely tuned active conformation—dependent on the αC-in arrangement, conserved lysine alignment, and activation loop/DFG motif dynamics—thereby destabilizing the active structural state and reducing TrkA's residual kinase activity and signaling efficiency[9, 18, 19].

Clinically, this N-lobe perturbation correlates with markedly reduced NGF-induced TrkA autophosphorylation and downstream signaling via pERK and pAKT pathways. The attenuated NGF response corresponds to a different type of HSAN4, reflecting greater loss of NGF-TrkA signaling function. This impaired kinase activity compromises intracellular cascade activation essential for neuronal survival and differentiation[18, 20, 21].

The αC-helix/Lys region is fundamental to kinase activation, as the αC-in conformation stabilizes the catalytic lysine required for ATP coordination and phosphotransfer. Destabilizing variants such as p.His569Gln disrupt these interactions, reducing kinase activity and impairing TrkA autophosphorylation. This attenuates downstream MAPK/ERK and PI3K/AKT signaling, compromising neuronal development and pain perception[22, 23]. Thus, p.His569Gln compromises structural integrity critical for TrkA activation, attenuating NGF signaling and producing a different HSAN4 phenotype. This molecular mechanism is consistent with the pronounced reduction in NGF stimulus response observed in affected patients. The p.His569Gln mutation increases TrkA stability (ΔΔG_stability 0.37 kcal·mol^{-1}), yet this gain may paradoxically impair function. TrkA kinase activity depends on dynamic conformational changes rather than a rigid structure; excessive stabilization restricts the flexibility required for NGF-induced conformational transitions. This reflects the "stability-function trade-off," whereby both insufficient and excessive stabilization can compromise protein function[23, 24]. His569 occupies a critical position within the TrkA kinase domain, adjacent to the kinase insert domain (KID)—a structural feature underlying the functional divergence between TrkA and TrkB. Substitution with glutamine, a polar residue capable of extended interactions, may sterically hinder substrate access or disrupt catalytic cycle dynamics[25]. Additionally, p.His569Gln may induce endoplasmic reticulum misfolding, subjecting TrkA to stringent quality control and targeting the misfolded receptor for degradation via the ubiquitin-proteasome system or autophagy[26, 27]. This would substantially reduce the cellular pool of usable TrkA protein. Given that the patient exhibits excessive sweating rather than an inability to sweat, this presentation may warrant revising the diagnosis to "Congenital Insensitivity to Pain with or without Anhidrosis."

Glu590 is a critical residue of the ATP-binding hinge region in the NTRK1 kinase domain, situated at the interface of the N- and C-terminal lobes. Structural data show that inhibitors anchor to the ATP-binding pocket via two to three hydrogen bonds with the backbone carbonyl groups of Glu590 and adjacent Met592. Notably, these interactions are backbone-mediated, targeting the carbonyl oxygen rather than the side chain directly[28, 29]. The p.Glu590Gln variant exerts a hypomorphic rather than loss-of-function effect on NTRK1. Although the hinge region is critical for ATP binding, most contacts are backbone-mediated, rendering them relatively insensitive to side-chain substitution. The Glu590Gln change—replacing a negatively charged residue with a polar, uncharged one—subtly alters local polarity and water networks without disrupting the overall kinase fold or architecture[30–32].

Rotamer analysis showed that Gln590 tolerates multiple acceptable conformations with minimal structural strain, suggesting local modulation of interactions without global fold disruption or complete loss of ATP binding—supporting partial retention of kinase function consistent with a hypomorphic

effect. This tolerance is characteristic of hinge-region variants in tyrosine kinases, where backbone-mediated ATP contacts predominate and side-chain substitutions are generally well tolerated unless key hydrogen bonds or overall conformation are disrupted[33, 34]. The variant likely induces subtle shifts in local polarity and hydration, modulating binding dynamics while preserving overall kinase architecture and residual activity. Although direct literature on p.Glu590Gln is limited, this interpretation aligns with the broader understanding of hinge-region mutations, where side-chain alterations near the ATP-binding site produce variable effects—from complete inactivation to mild functional modulation—depending on structural context; the identification of acceptable rotamers in silico supports a hypomorphic rather than a loss-of-function or dominant-negative outcome[32, 34]. Thus, p.Glu590Gln preserves the major structural features of the kinase hinge region while subtly modulating local polarity and hydration, permitting residual ATP binding and kinase activity, consistent with the patients' clinical presentation.

The c.1177 + 2T > A variant disrupts the canonical GU dinucleotide at the + 2 position of the 5' splice donor site—a nearly invariant sequence conserved across human and yeast systems due to splicing chemistry and U1/U6 snRNA interactions—markedly reducing U1 snRNP binding stability and inhibiting spliceosome assembly[35, 36]. The + 2 T > A variant thus represents a core splicing defect, directly disrupting the conserved GU motif at the first step of spliceosome assembly. Large-cohort analyses using tools such as MaxEntScan and SpliceAI show strong correlations between absolute delta scores and pathogenicity, particularly at canonical donor and acceptor positions; here, the MaxEntScan score dropped from 5.196 (wild-type) to − 2.987 (mutant), a Δ − 8.183 loss, a profile typical of pathogenic variants indicating severe attenuation of the 5' donor signal[16]. A SpliceAI delta donor loss score of 0.97 indicates that this variant will almost certainly (97% probability) cause splice alteration at the relevant locus; in published evaluations, scores above 0.5 are classified as strongly pathogenic, and scores above 0.8–0.9 as highly pathogenic[15]. The “high impact” signal from these two independent algorithms supports the idea that c.1177 + 2T > A largely eliminates the canonical 5' donor usage and creates a significant splicing defect.

In splice biology, + 1/+2 mutations at canonical 5' donor sites typically produce one of three aberrant outcomes—cryptic donor activation, exon skipping, or intron retention—mechanisms similarly documented for NTRK1 (Fig. 3). The three outcomes predicted for c.1177 + 2T > A are consistent with these established patterns, typically yielding transcripts subject to NMD or severely truncated, non-functional proteins; splice-site mutations are well documented in HSAN4/CIPA cohorts and are frequently associated with severe phenotypes[2, 17, 37]. Notably, the intronic c.851-33T > A variant represents a recognized hotspot mutation recurrently identified in Japanese and Han Chinese populations, detected in 63.8% of Han Chinese HSAN4/CIPA patients in one study[17]. In vitro splicing analyses by Miura et al. demonstrated that c.935–33T > A disrupts the intron 7 branch point, generating a 137 bp aberrant insertion through partial intron retention and producing a truncated TrkA protein[38]. Homozygous carriers present with severe early-onset HSAN4/CIPA, while compound heterozygotes with c.851-33T > A and a missense variant typically show milder phenotypes. Canonical + 1/+2 splice site mutations dramatically reduce functional TrkA via exon skipping or aberrant transcripts, yielding severe presentations, whereas deep intronic or branch point mutations permit residual normal splicing and

exhibit greater phenotypic variability[17, 37]. In conclusion, c.1177 + 2T > A represents a near-complete loss-of-function splice defect consistent with a severe HSAN4/CIPA phenotype, supported by disruption of a highly conserved canonical donor position, near-complete donor loss predicted by robust computational tools, and clinical and molecular patterns concordant with other pathogenic *NTRK1* splice-site mutations.

NTRK1 knockdown in mice causes cognitive impairment, hippocampal neuronal damage, and exacerbated depression-like behavior, linked to suppressed mitophagy and inactivation of the AMPK/ULK1/FUNDC1 pathway[39] —consistent with the impulse control disorder observed in Patient P1.

As for what is currently known on this subject, the location of *NTRK1* mutations within the protein appears to be associated with phenotypic severity: mutations affecting critical functional domains tend to produce more severe symptoms and intellectual disability, whereas peripheral mutations are associated with milder phenotypes. However, there are 13 variants in the ClinVar database whose clinical significance is unknown but evidence for genotype-phenotype correlations remains limited, and functional validation has not been performed for most variants[40, 41]. Although severe intellectual disability has been reported in a patient from northern Han China homozygous for c.851-33T > A, clinical severity may vary among other carriers of the same variant[17]. In the study by Geng et al., all probands carried *NTRK1* mutations, as homozygotes or compound heterozygotes, and the study identified two novel repeat mutations along with aberrant splicing (exon 2 skipping)[42]. In the case reported by Kurth et al., uniparental disomy converted an intronic variant that was heterozygous in the parents into a homozygous state in the patient; this variant created a new splice site, incorporating 10 intronic bases into the mRNA and producing a non-functional gene product[43]. Indo has identified the c.1660delC and c.2020G > T variants in the Japanese population[4]. Shatzky et al. identified the c.1860–1861insT (NM_001012331.1) (NP_001012331.1) variant as the founder variant in Israeli Bedouins[44]. Tüysüz et al. identified the c.1633-1G > T (c.1615-1G > T) variant as a founder variant in the Turkish population and described aberrant splicing in which exon 14 is skipped[45].

If we consider what this study contributes to this topic, holistic evaluation of the three *NTRK1* variants indicates that phenotypic heterogeneity in HSAN4/CIPA arises from qualitative differences in their molecular mechanisms;

1. 1. p.His569Gln increases TrkA stability, as confirmed by DynaMUT2, expanding its interaction network and rigidifying the local environment; this restricts the conformational flexibility required for NGF response, yielding a severe loss-of-function profile.
2. 2. p.Glu590Gln, by contrast, shows a hypomorphic, partial loss-of-function profile, with rotamer-level rearrangements subtly altering side-chain polarity and local hydration while preserving the backbone ATP-binding motifs, consistent with its milder clinical presentation. 3. The c.1177 + 2T > A variant disrupts the canonical GU motif at the + 2 splice-donor position, causing a severe splicing defect that nearly abolishes normal *NTRK1* transcript processing, as supported by markedly reduced

MaxEntScan and SpliceAI scores; like other *NTRK1* donor-site mutations, which typically cause frameshift, nonsense-mediated decay, or severe truncation, this variant likely represents a functionally null or near-null allele.

Conclusion

These three variants demonstrate that clinical severity in HSAN4/CIPA correlates not merely with mutation presence, but with its location, molecular consequence, and functional outcome. These findings should be interpreted in light of several limitations. Structural models and rotamer scans are static and model-dependent, and cannot capture receptor dynamics, solvent effects, cellular transport, or allosteric signaling; results are therefore limited to clinical characterization and computational prioritization of experimentally testable hypotheses. Moreover, *NTRK1* genotype-phenotype correlations remain poorly understood and largely unvalidated functionally, despite several population-specific founder variants identified worldwide that often cause disease through aberrant splicing. Simply documenting such mutations is no longer sufficient; this evidence must now be strengthened through protein modeling.

Declarations

The authors declare that no funds, grants, or other support were received during the preparation of this manuscript. The authors have no relevant financial or non-financial interests to disclose. All authors contributed to the study conception and design. Material preparation, data collection and analysis were performed by Aydeniz Aydin Gumus, Serdar Bozlak, Merve Cakmak, Peren Perk and Melih Civan. The first draft of the manuscript was written by Aydeniz Aydin Gumus and Ekrem Akbulut and all authors commented on previous versions of the manuscript. All authors read and approved the final manuscript. This study was performed in line with the principles of the Declaration of Helsinki. Approval was granted by the Ethics Committee of of Başakşehir Çam and Sakura City Hospital on June 5, 2026 (Ref. No. KAEK/06.05.2026.265; approval no. E-96317027-515.10-315606544). Informed consent was obtained from all individual participants included in the study.

Author Contribution

Material preparation, data collection and analysis were performed by A.A.G., S.B., M. C., P.P.and M.C. The first draft of the manuscript was written by AAG and E.A. .All Figures were prepared by E.A. All authors commented on previous versions of the manuscript.

References

1. Indo Y (2002) Genetics of congenital insensitivity to pain with anhidrosis (CIPA) or hereditary sensory and autonomic neuropathy type IV. Clinical, biological and molecular aspects of mutations

in TRKA(NTRK1) gene encoding the receptor tyrosine kinase for nerve growth…. Clin Auton Res. https://doi.org/10.1007/S102860200016. 12 Suppl 1

2. Li L, Jia C, Tang Y et al (2021) Novel Gross Deletion Mutations in NTRK1 Gene Associated With Congenital Insensitivity to Pain With Anhidrosis. Front Pediatr 9. https://doi.org/10.3389/fped.2021.638190
3. Indo Y (2009) Nerve growth factor, interoception, and sympathetic neuron: Lesson from congenital insensitivity to pain with anhidrosis. Auton Neurosci 147:3–8. https://doi.org/10.1016/J.AUTNEU.2009.01.008
4. Indo Y (2001) Molecular basis of congenital insensitivity to pain with anhidrosis (CIPA): mutations and polymorphisms in TRKA (NTRK1) gene encoding the receptor tyrosine kinase for nerve growth factor. Hum Mutat 18:462–471. https://doi.org/10.1002/HUMU.1224
5. Barker PA, Mantyh P, Arendt-Nielsen L et al (2020) Nerve growth factor signaling and its contribution to pain. J Pain Res 13:1223–1241. https://doi.org/10.2147/JPR.S247472
6. Masson E, Zou W, Bin, Génin E et al (2022) Expanding ACMG variant classification guidelines into a general framework. Hum Genomics 16. https://doi.org/10.1186/s40246-022-00407-x
7. Biasini M, Bienert S, Waterhouse A et al (2014) SWISS-MODEL: Modelling protein tertiary and quaternary structure using evolutionary information. Nucleic Acids Res 42. https://doi.org/10.1093/nar/gku340
8. Abramson J, Adler J, Dunger J et al (2024) Accurate structure prediction of biomolecular interactions with AlphaFold 3. Nature 630:493–500. https://doi.org/10.1038/s41586-024-07487-w
9. Bertrand T, Kothe M, Liu J et al (2012) The Crystal Structures of TrkA and TrkB Suggest Key Regions for Achieving Selective Inhibition. J Mol Biol 423:439–453. https://doi.org/10.1016/J.JMB.2012.08.002
10. Wehrman T, He X, Raab B et al (2007) Structural and Mechanistic Insights into Nerve Growth Factor Interactions with the TrkA and p75 Receptors. Neuron 53:25–38. https://doi.org/10.1016/j.neuron.2006.09.034
11. Stachel SJ, Sanders JM, Henze DA et al (2014) Maximizing Diversity from a Kinase Screen: Identification of Novel and Selective pan-Trk Inhibitors for Chronic Pain. J Med Chem 57:5800–5816. https://doi.org/10.1021/JM5006429
12. Wiederstein M, Sippl MJ (2007) ProSA-web: interactive web service for the recognition of errors in three-dimensional structures of proteins. Nucleic Acids Res 35:W407–W410. https://doi.org/10.1093/NAR/GKM290
13. Chen VB, Arendall WB, Headd JJ et al (2009) MolProbity: all-atom structure validation for macromolecular crystallography. urn:issn:0907–4449 66. 12–21. https://doi.org/10.1107/S0907444909042073
14. Rodrigues CHM, Pires DEV, Ascher DB (2021) DynaMut2: Assessing changes in stability and flexibility upon single and multiple point missense mutations. Protein Sci 30:60–69. https://doi.org/10.1002/pro.3942

15. de Sainte Agathe JM, Filser M, Isidor B et al (2023) SpliceAI-visual: a free online tool to improve SpliceAI splicing variant interpretation. Hum Genomics 2023 17:1. https://doi.org/10.1186/S40246-023-00451-1
16. Yeo G, Burge CB (2003) Maximum entropy modeling of short sequence motifs with applications to RNA splicing signals. Proceedings of the Annual International Conference on Computational Molecular Biology, RECOMB 322–331. https://doi.org/10.1145/640075.640118;WGROUP:STRING:ACM
17. Li N, Guo S, Wang Q et al (2019) Heterogeneity of clinical features and mutation analysis of NTRK1 in Han Chinese patients with congenital insensitivity to pain with anhidrosis. J Pain Res 12:453–465. https://doi.org/10.2147/JPR.S188566
18. Herrmann JL, Menter DG, Hamada JI et al (2017) Mediation of NGF-stimulated extracellular matrix invasion by the human melanoma low-affinity p75 neurotrophin receptor: melanoma p75 functions independently of trkA. 1205–1216. https://doi.org/101091/mbc4111205 4
19. Russo M, Misale S, Wei G et al (2016) Acquired resistance to the TRK inhibitor entrectinib in colorectal cancer. Cancer Discov 6:36–44. https://doi.org/10.1158/2159-8290.CD-15-0940/42485/.AM/ACQUIRED-RESISTANCE-TO-THE-TRK-INHIBITOR
20. Moraes BC, Ribeiro-Filho HV, Roldão AP et al (2022) Structural analysis of TrkA mutations in patients with congenital insensitivity to pain reveals PLCγ as an analgesic drug target. Sci Signal 15. https://doi.org/10.1126/SCISIGNAL.ABM6046;SUBPAGE:STRING:FULL
21. Khaled B, Alzahayqa M, Jaffal A et al (2023) Identification of founder and novel mutations that cause congenital insensitivity to pain (CIP) in palestinian patients. BMC Med Genomics 2023 16(1):120. https://doi.org/10.1186/S12920-023-01544-5
22. Duan L, Hope JM, Guo S et al (2018) Optical Activation of TrkA Signaling. ACS Synth Biol 7:1685–1693. https://doi.org/10.1021/ACSSYNBIO.8B00126
23. Socha RD, Tokuriki N (2013) Modulating protein stability - Directed evolution strategies for improved protein function. FEBS J 280:5582–5595. https://doi.org/10.1111/FEBS.12354;ISSUE:ISSUE:DOI
24. Teufl M, Zajc CU, Traxlmayr MW (2022) Engineering Strategies to Overcome the Stability–Function Trade-Off in Proteins. ACS Synth Biol 11:1030–1039. https://doi.org/10.1021/ACSSYNBIO.1C00512
25. Artim SC, Kiyatkin A, Lemmon MA (2020) Comparison of tyrosine kinase domain properties for the neurotrophin receptors TrkA and TrkB. Biochem J 477:4053–4070. https://doi.org/10.1042/BCJ20200695
26. Franco ML, Melero C, Sarasola E et al (2016) Mutations in TrkA causing congenital insensitivity to pain with anhidrosis (CIPA) induce misfolding, aggregation, and mutation-dependent neurodegeneration by dysfunction of the autophagic flux. J Biol Chem 291:21363–21374. https://doi.org/10.1074/jbc.M116.722587
27. Haidar M, Timmerman V (2017) Autophagy as an emerging common pathomechanism in inherited peripheral neuropathies. Front Mol Neurosci 10:270143. https://doi.org/10.3389/FNMOL.2017.00143/FULL

28. Yan W, Lakkaniga NR, Carlomagno F et al (2018) Insights into Current Tropomyosin Receptor Kinase (TRK) Inhibitors: Development and Clinical Application. J Med Chem 62:1731–1760. https://doi.org/10.1021/ACS.JMEDCHEM.8B01092
29. Qin Q, Guo Z, Lu S et al (2024) Discovery of novel 3-(1H-pyrazol-4-yl)-1H-indazole derivatives as potent type II TRK inhibitors against acquired resistance. Eur J Med Chem 264:115953. https://doi.org/10.1016/J.EJMECH.2023.115953
30. El-Nassan HB (2024) Current landscape of tropomyosin receptor tyrosine kinase inhibitors. Future Med Chem 16:1945–1948. https://doi.org/10.1080/17568919.2024.2403968
31. Ghose AK, Herbertz T, Pippin DA et al (2008) Knowledge Based Prediction of Ligand Binding Modes and Rational Inhibitor Design for Kinase Drug Discovery. J Med Chem 51:5149–5171. https://doi.org/10.1021/JM800475Y
32. Zhang H, He F, Gao G et al (2023) Approved Small-Molecule ATP-Competitive Kinases Drugs Containing Indole/Azaindole/Oxindole Scaffolds: R&D and Binding Patterns Profiling. Molecules 2023, Vol 28, Page 943 28:943. https://doi.org/10.3390/MOLECULES28030943
33. Zhao Z, Bourne PE (2023) How Ligands Interact with the Kinase Hinge. ACS Med Chem Lett 14:1503–1508. https://doi.org/10.1021/ACSMEDCHEMLETT.3C00212
34. Xing L, Klug-Mcleod J, Rai B, Lunney EA (2015) Kinase hinge binding scaffolds and their hydrogen bond patterns. Bioorg Med Chem 23:6520–6527. https://doi.org/10.1016/J.BMC.2015.08.006
35. White DS, Dunyak BM, Vaillancourt FH, Hoskins AA (2024) A sequential binding mechanism for 5' splice site recognition and modulation for the human U1 snRNP. Nature Communications 2024 15:1 15:8776-. https://doi.org/10.1038/s41467-024-53124-5
36. Hansen SR, White DS, Scalf M et al (2022) Multi-step recognition of potential 5’ splice sites by the Saccharomyces cerevisiae U1 snRNP. https://doi.org/10.7554/ELIFE.70534. Elife 11:
37. Sun L, Dai J, Zhang Y et al (2024) A novel NTRK1 splice site variant causing congenital insensitivity to pain with anhidrosis in a Chinese family. Front Genet 15:1345081. https://doi.org/10.3389/FGENE.2024.1345081/TEXT
38. Miura Y, Mardy S, Awaya Y et al (2000) Mutation and polymorphism analysis of the TRKA (NTRK1) gene encoding a high-affinity receptor for nerve growth factor in congenital insensitivity to pain with anhidrosis (CIPA) families. Human Genetics 1999 106:1 106:116–124. https://doi.org/10.1007/S004399900205
39. Nakajima K, Miranda A, Craig DW et al (2020) Ntrk1 mutation co-segregating with bipolar disorder and inherited kidney disease in a multiplex family causes defects in neuronal growth and depression-like behavior in mice. Translational Psychiatry 2020 10(1 10):407–. https://doi.org/10.1038/s41398-020-01087-8
40. Liu Z, Liu J, Liu G et al (2018) Phenotypic heterogeneity of intellectual disability in patients with congenital insensitivity to pain with anhidrosis: A case report and literature review. J Int Med Res 46:2445–2457. https://doi.org/10.1177/0300060517747164

41. Li S, Hu H, ying, Xu JJ et al (2021) Identification of novel variations in the NTRK1 gene causing congenital insensitivity to pain with anhidrosis. Mol Genet Genomic Med 9:e1839. https://doi.org/10.1002/MGG3.1839
42. Geng X, Liu Y, Ren XZ et al (2018) Novel NTRK1 mutations in Chinese patients with congenital insensitivity to pain with anhidrosis. Mol Pain 14. https://doi.org/10.1177/1744806918781140
43. Kurth I, Baumgartner M, Schabhüttl M et al (2016) Whole exome sequencing in congenital pain insensitivity identifies a novel causative intronic NTRK1-mutation due to uniparental disomy. Am J Med Genet Part B: Neuropsychiatric Genet 171:875–878. https://doi.org/10.1002/AJMG.B.32458
44. Mardy S, Miura Y, Endo F et al (2001) Congenital insensitivity to pain with anhidrosis (CIPA): Effect of TRKA (NTRK1) missense mutations on autophosphorylation of the receptor tyrosine kinase for nerve growth factor. Hum Mol Genet 10:179–188. https://doi.org/10.1093/hmg/10.3.179
45. Tüysüz B, Bayrakli F, Diluna ML et al (2008) Novel NTRK1 mutations cause hereditary sensory and autonomic neuropathy type IV: demonstration of a founder mutation in the Turkish population. Neurogenetics 9:119–125. https://doi.org/10.1007/S10048-008-0121-9

Figures

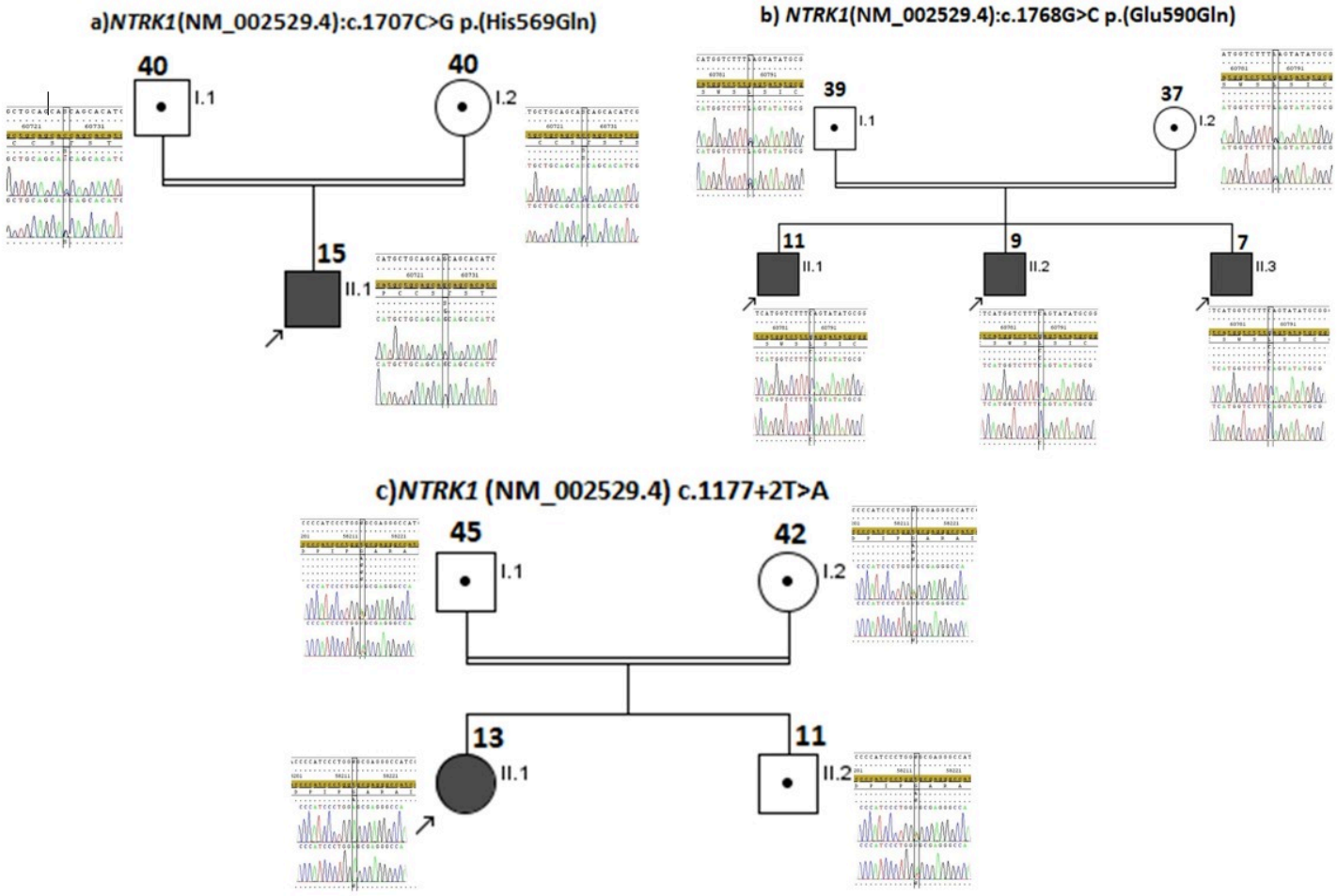


Figure 1

Sanger sequencing of *NTRK1* mutations in patients and results of familial segregation analysis

a) Pedigree of patient P1

b) Pedigree of siblings P2, P3, and P4

c) Pedigree of patient P5

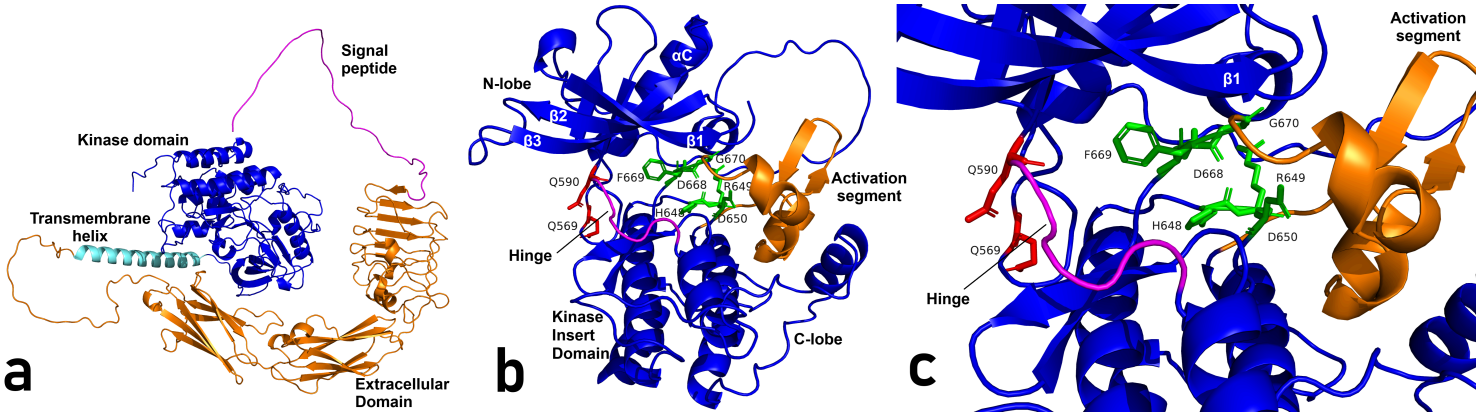


Figure 2

Illustration of the homology model of the TrkA protein.

a) Cartoon representation of the domain structure of the mutant TrkA protein (magenta: signal peptide, orange: extracellular domain, aquamarine: transmembran helix, blue: protein kinase domain), b) Functional and structural regions of the kinase domain of the mutant TrkA protein, c) Key structural motifs of the kinase domain of TrkA protein (Hinge: It is a short segment connecting the N- and C-lobes of the kinase. The adenine ring of ATP and many inhibitors are "anchored" here, mostly by forming 1–3 hydrogen bonds with backbone carbonyl/amide atoms. Therefore, the hinge is critical for ATP/inhibitor binding and selectivity; changes around the hinge can affect binding affinity and drug sensitivity. HRD motif (His-Arg-Asp; catalytic loop): It is part of the catalytic core of the active site. Specifically, Asp contributes to the correct execution of phosphate transfer chemistry and the proper alignment of the substrate's –OH group to be phosphorylated. If the HRD motif is disrupted, kinase activity is usually severely reduced. DFG motif (Asp-Phe-Gly; activation loop initiation): It is one of the "on/off" switches of the kinase. Asp is essential for Mg^{2+} binding/stabilization of ATP phosphates in most kinases; Phe acts as a hydrophobic switch determining the conformation. The DFG-in (active) and DFG-out (often inactive) conformations determine both activation and the binding pattern of certain inhibitors)

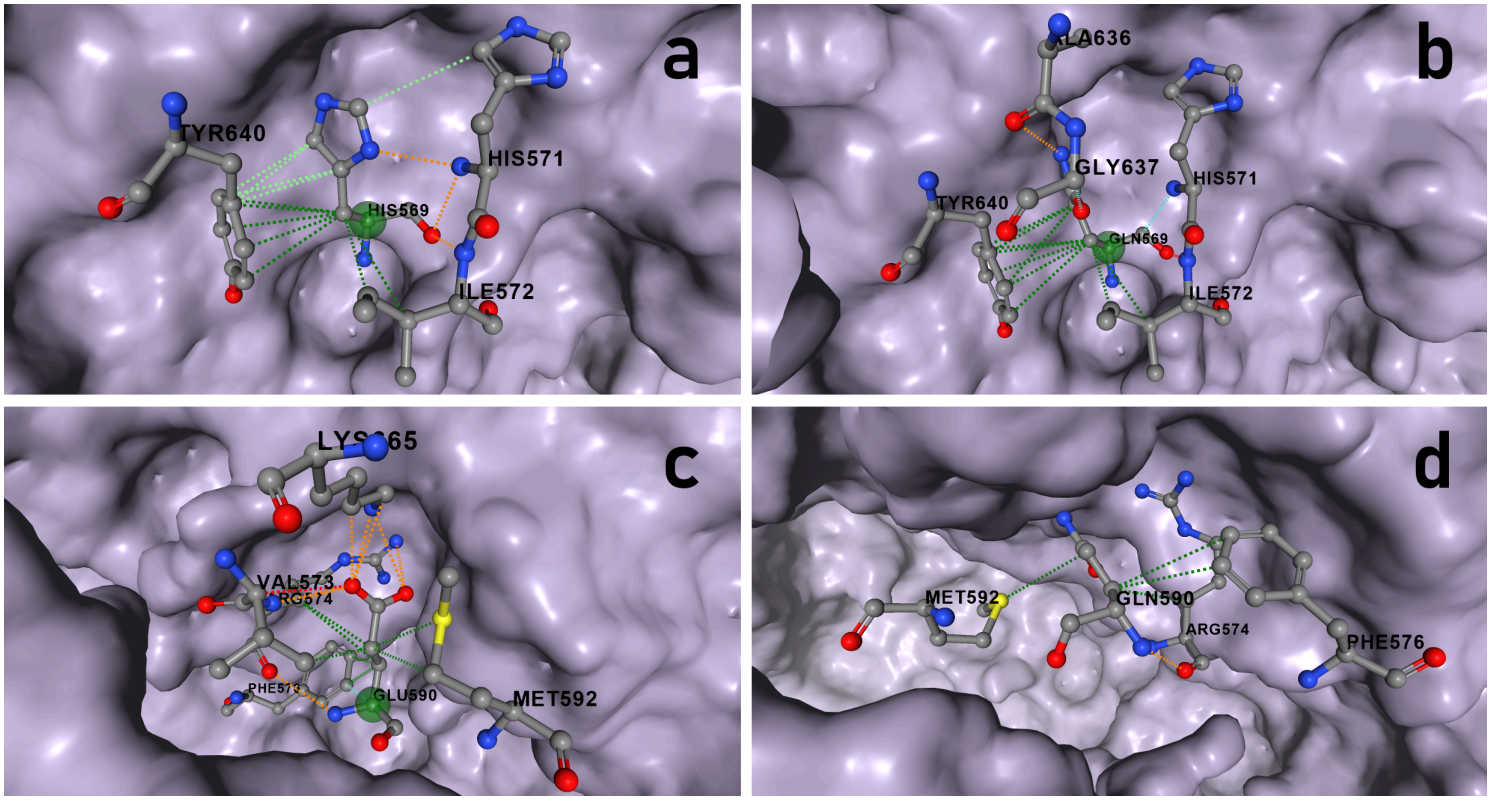


Figure 3

The changes in the atomic interaction network in the TrkA protein structure caused by the p.His569Gln and p.Glu590Gln mutations of *NTRK1* (The colors of the line represent; dark green-hydrophobic, light green-aromatic, light blue van der Waals, orange-polar interaction, red-hydrogen bond).

a) Atomic interactions at position 569 in wild-type TrkA, b) Atomic interactions at position 569 in mutant TrkA, c) Atomic interactions at position 590 in wild-type TrkA, d) Atomic interactions at position 590 in mutant TrkA.

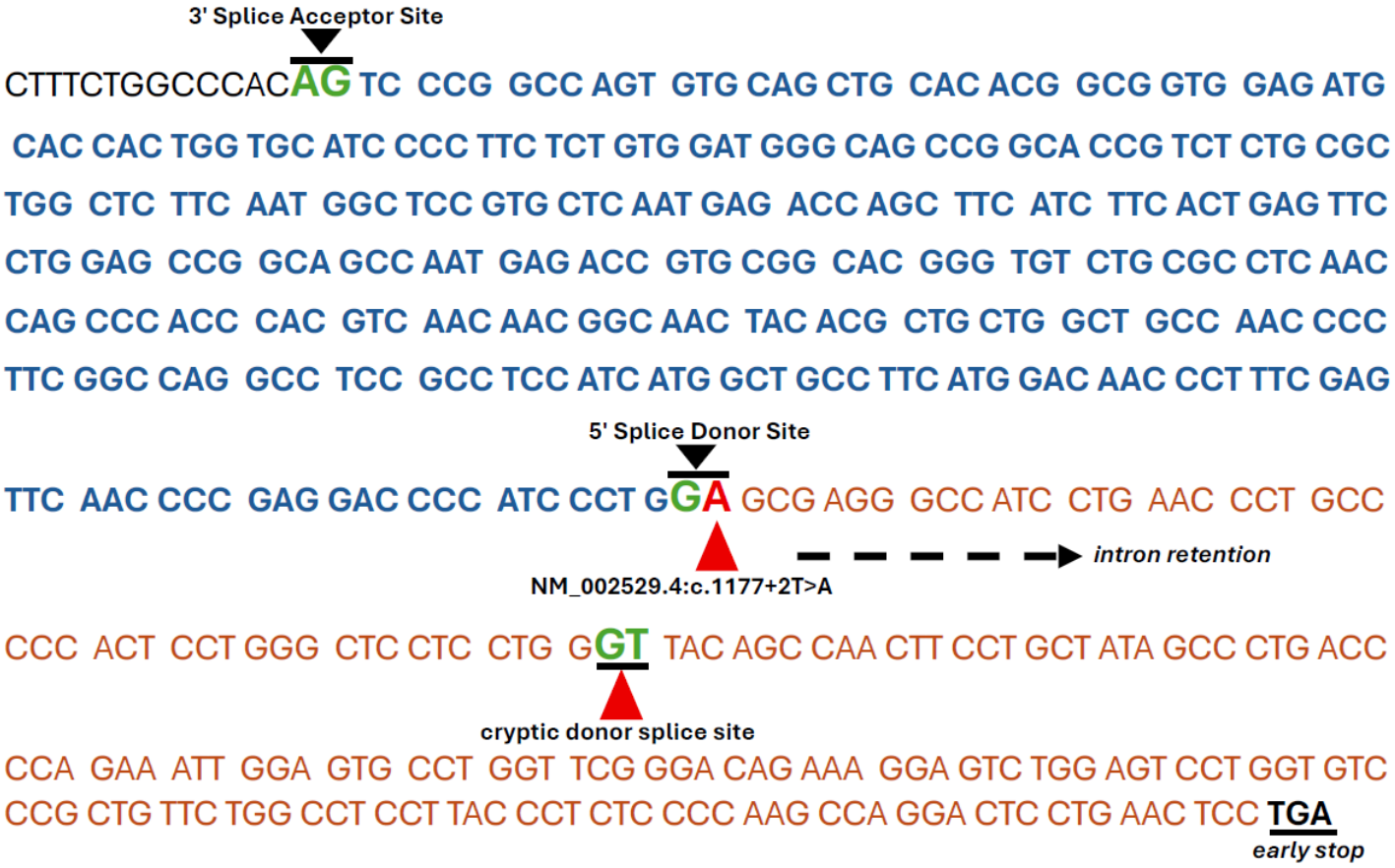


Figure 4

The c.1177+2T>A mutation of *NTRK1* disrupts the 5' splice donor site. The figure represents the changes this mutation can cause at the splice site.

Supplementary Files

This is a list of supplementary files associated with this preprint. Click to download.

- Tabless.docx